SOLAR ACTIVE REGIONS AT MILLIMETER WAVELENGTHS

M. R. KUNDU

Astronomy Program, University of Maryland, College Park, Md., U.S.A.

(Received 24 February, 1970)

Abstract. Some properties of solar active regions at 9, 3.5 and 1.2 mm wavelengths are discussed. The regions have excess brightness temperatures of up to 1000, 700 and 150 K at 9, 3.5 and 1.2 mm wavelengths. The background radiation at 3.5 mm is often seen to be 'absorbed' in regions closely coincident with Hα dark filaments on the disk. Interpretation of this 'absorption' as due to the large optical thickness of the overlying filamentary material leads to an estimate of electron density in the filaments. The 9 and 3.5 mm-λ regions show almost one-to-one correspondence with the Ca-plage regions as well as with the regions on magnetograms. The latter relationship suggests the possibility of measuring chromospheric magnetic fields from the measurement of polarization at millimeter wavelengths.

1. Introduction

High resolution observations of the Sun have been made at 9, 3.5 and 1.2 mm wavelengths during the period 15–30 September 1969, using the 36-foot radio telescope of the National Radio Astronomy Observatory*, situated at Kitt Peak in Tucson, Arizona. The half-power beamwidths of the telescope are 3'.5, 1'.2 and 1'.2 arc respectively at 9, 3.5 and 1.2 mm wavelengths. The telescope has an azimuth-elevation mount and has complete computer control of pointing, coordinate conversion and data acquisition. The telescope and the radiometers have been described previously (Buhl and Tlamicha, 1970). Good weather conditions and very little of equipment failure permitted us to make a total of about 40 solar maps at the three wavelengths. In this paper, we shall discuss some characteristic features of the active regions, and their relationships with the features observed at optical wavelengths.

2. Observations

The observations were taken by scanning the Sun in right ascension at the rate of 1° per minute, the successive scans being separated by 1′ of arc in declination. In order to provide sufficient baselines, the scans were chosen to be 45′ long and a total of 37 scans were taken with 1′ arc intervals. At 3.5 mm wavelength, for some maps a total of 76 scans with 0'.5 of arc intervals in declination between scans were also taken. This procedure was adopted in order to take full advantage of the angular resolution (1'.2 arc) available. The scan program for the telescope was set up to first scan east for 45′ arc and then reverse and scan west at the same declination, the data being recorded digitally in both directions; the data were also recorded on analog charts usually for the east scan only, and sometimes also for the west scan. The computer

* Operated by Associated Universities, Inc. under contract with the National Science Foundation.

Solar Physics **13** (1970) 348–356.

continuously calculates the interpolated position for the Sun and corrects for horizontal parallax and pointing errors. Consequently, a complete solar map consists of a 45′ by 37′ arc grid of data points, centered on the Sun, or in the case of some 3.5 mm maps a grid of 45′ by 38′ arc in R.A. and δ. The active regions were scanned repeatedly over a R.A. range of 30′ or 35′ arc and at declination intervals of 1′ arc over a suitable declination range in which one or more dominant active regions were located. These scans were repeated at time intervals of approximately d min, where d is the declination range in arc minutes.

Because of the difficulty of obtaining an absolute temperature calibration, or of determining accurately the beam efficiency (approximately 75% as measured on the moon at 3.5 mm-λ) of the antenna we have assumed mean temperatures of 6000 K, 6400 K an 7000 K respectively at 1.2, 3.5 and 9 mm wavelengths respectively. Since the efficiency is lower for sources smaller than the Sun, the temperature differences between hot and cold regions may be underestimated. After scaling the data to the appropriate mean quiet Sun temperatures at different wavelengths, the data points were plotted on a Calcomp plotter using the available contour mapping program of NRAO. On the solar disk, 50 K contour intervals were chosen to display the solar activity. Contour intervals of 500 K were used near the limbs of the Sun where the temperature changes very rapidly. Contour temperatures are printed out automatically and temperature depressions are indicated by small dashes in the direction of temperature decrease. Baseline contours set at 100 K are useful in displaying the behavior of the antenna off the sun. As has been pointed out by Buhl and Tlamicha (1970), the antenna beam seems to have no large discrete sidelobes at 3.5 mm-λ, and that the beam appears to be symmetrical in the azimuth and elevation planes to about 10%. The antenna performance seems to be better at 9 mm-λ, as can be judged from the much neater maps at 9 mm-λ as compared to those at 3.5 mm-λ. The limited number of solar maps indicate that the antenna side lobe structure is not much worse at 1.2 mm-λ.

In order to minimize atmospheric attenuation, measurements were made close to transit whenever possible. For off-transit observations, the individual scans were normalized with respect to a particular scan, namely the scan through the center of the Sun, by observing the latter at regular intervals of elevation angles. From measurements of this central scan at different elevation angles, an extinction curve was plotted for each day and all the scans were corrected by means of this extinction curve. The correction for atmospheric effect is particularly important for 1.2 mm observations; it is only slightly important at 3.5 mm, and is relatively unimportant at 9 mm wavelengths.

3. Results and Discussion

Figure 1 shows typical examples of solar maps at 9, 3.5 and 1.2 mm wavelengths. The maps at 9 and 3.5 mm shown in Figure 1 were taken on the same day. A comparison of these maps together with the corresponding maps in Hα and Ca II, as well as the Mt. Wilson magnetograms leads us to make the following conclusions:

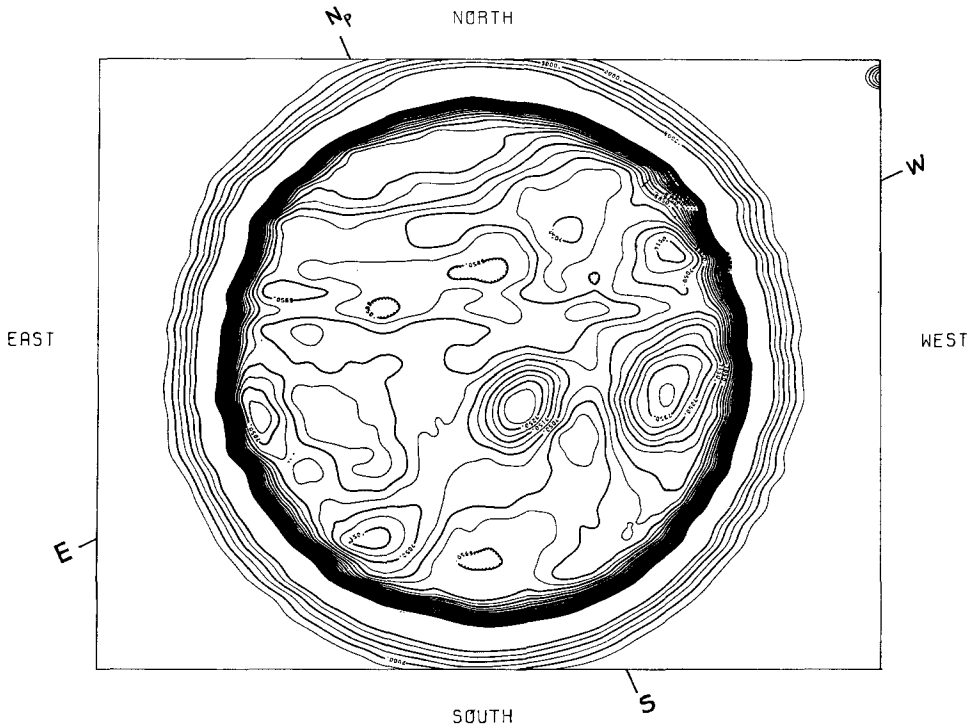

Fig. 1a. Solar map at 9 mm-λ for 17 September, 1969. The grid used was 45′ by 37′ in R.A. and δ at intervals of 1′ arc in δ.

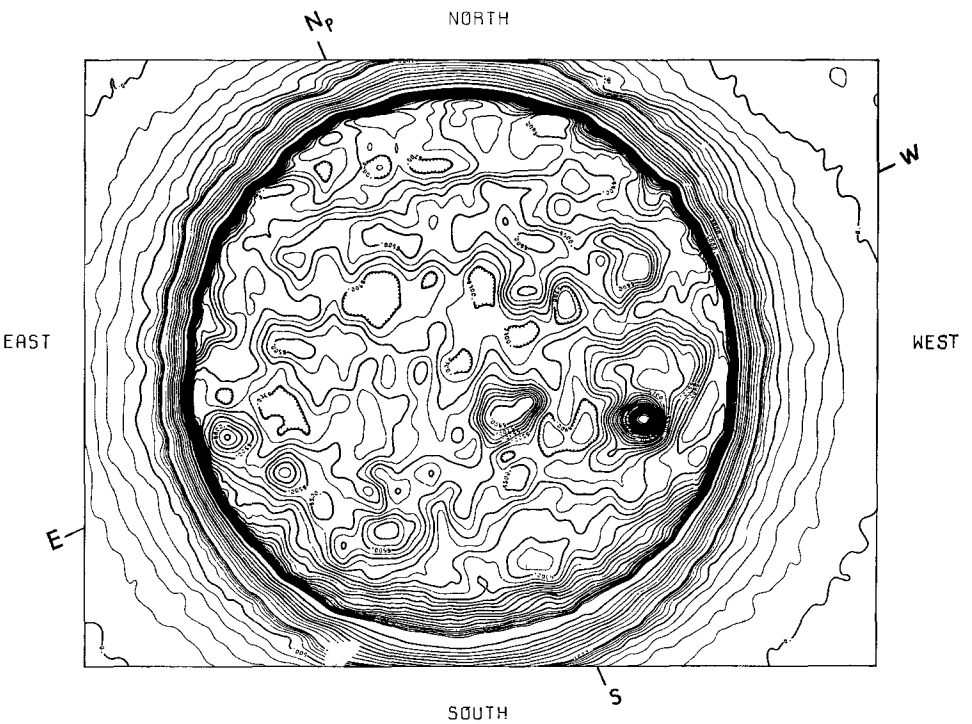

Fig. 1b. Solar map at 3.5 mm-λ for 17 September, 1969. The grid used was 45′ by 37′ in R.A. and δ at intervals of 1′ arc in δ.

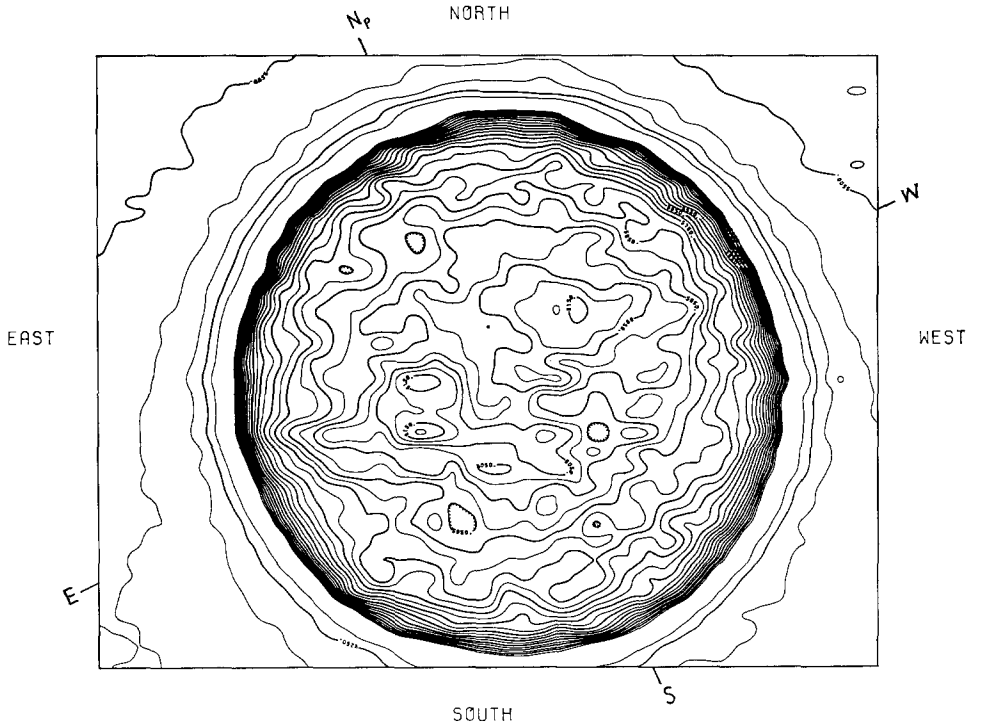

Fig. 1c. Solar map at 1.2 mm-λ for 25 September, 1969. The grid used was 45′ by 37′ in R.A. and δ at intervals of 1′ arc in δ.

(1) The maps at 3.5 and 9 mm are quite similar, although the maps at 3.5 mm show considerably more structure than the 9 mm maps, obviously due to higher angular resolution. The maps at 9 and 3.5 mm both show sources whose peak excess brightness temperatures can reach up to 1000 K and 700 K respectively, representing about 10–15% of the quiet Sun radiation at these wavelengths. The discrete sources at 9 and 3.5 mm are distributed practically all over the disk. Such a distribution is typical of Calcium plage regions. Indeed the 9 and 3.5 mm regions have very close correspondence in size and intensity with the plage regions. The intense sources at both 9 and 3.5 mm usually appear in pairs; these correspond to bipolar regions on magnetograms. A complex region at 3.5 mm consisting of three or more components usually corresponds to an equally complex region on magnetograms. Such complex structure is greatly smoothed out on the 9 mm maps because of lower resolution, although the existence of several components can often be discerned. Figure 2 shows the magnetogram which should be compared with the 3.5 and 9 mm maps of Figures 1a and 1b. The very close correspondence (almost 100%) between the mm regions and the magnetic regions is quite clear. The relationships between the millimeter wave regions, and the Ca-plage regions as well as the magnetic regions are shown in Figure 3. It is clear that the size of the mm regions is very closely related to the Ca-plage regions as well as the magnetic regions. It should be noted that for the radio regions we have

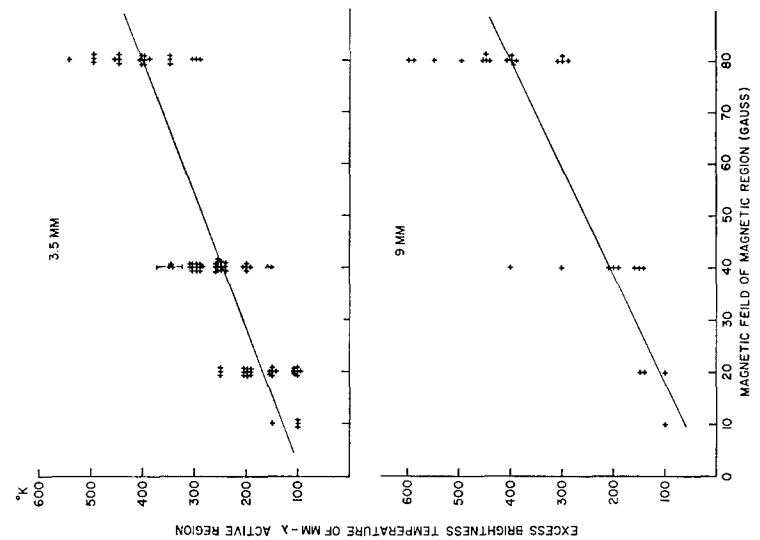

Fig. 3c

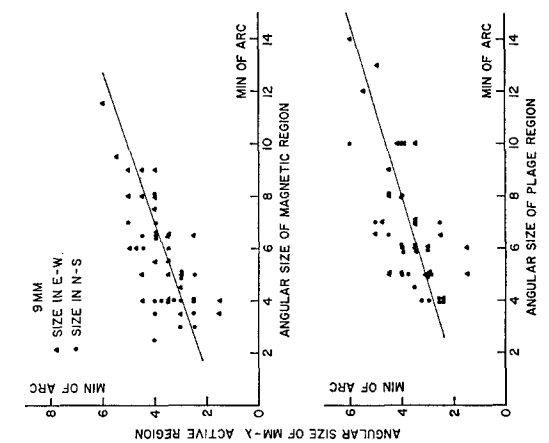

Fig. 3b

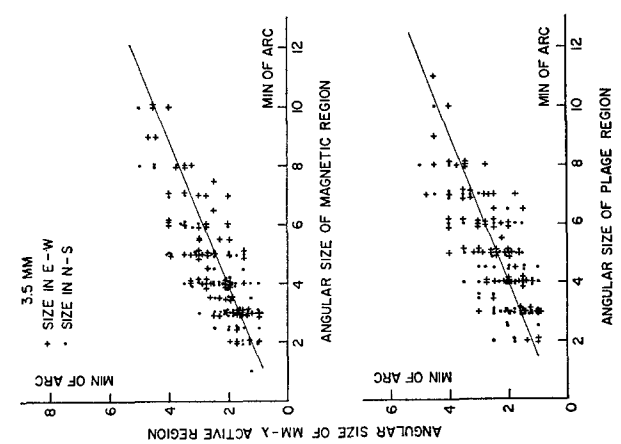

Fig. 3a

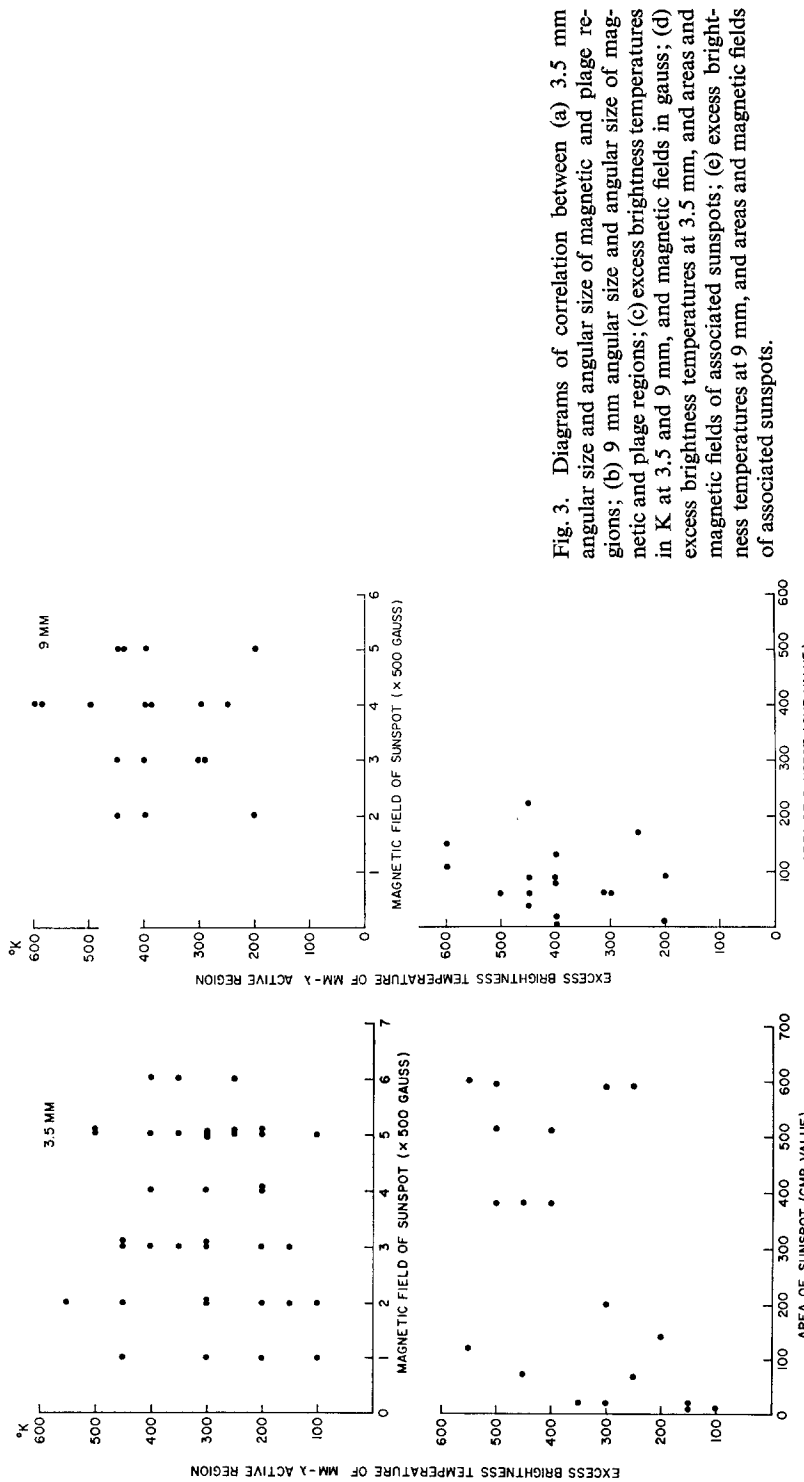

Fig. 3d

Fig. 3e

Fig. 3. Diagrams of correlation between (a) 3.5 mm angular size and angular size of magnetic and plage regions; (b) 9 mm angular size and angular size of magnetic and plage regions; (c) excess brightness temperatures in K at 3.5 and 9 mm, and magnetic fields in gauss; (d) excess brightness temperatures at 3.5 mm, and areas and magnetic fields of associated sunspots; (e) excess brightness temperatures at 9 mm, and areas and magnetic fields of associated sunspots.

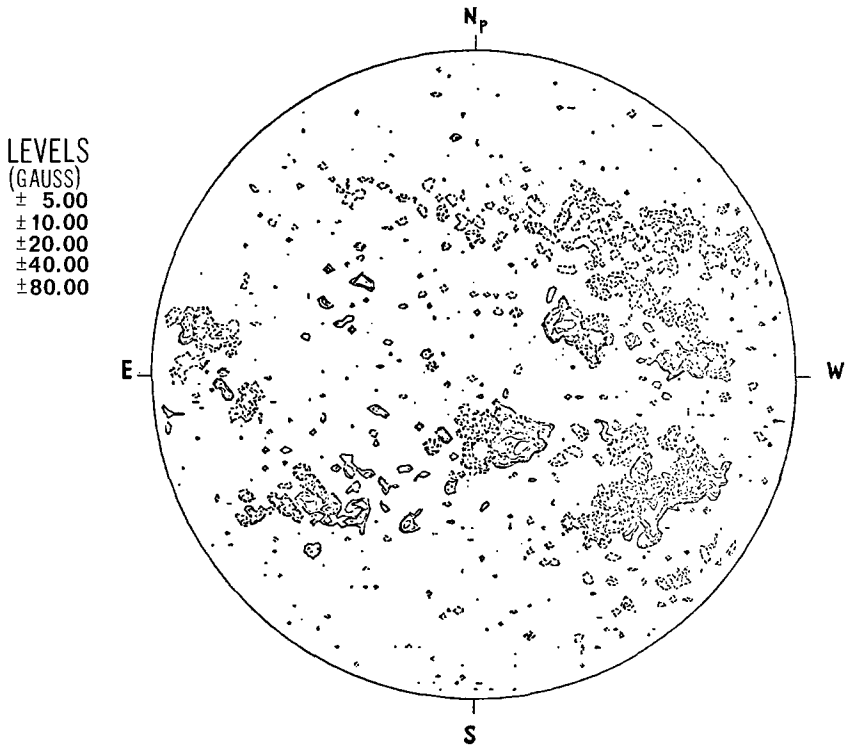

Fig. 2. Mount Wilson magnetogram for 17 September, 1969.

taken only the half-power width of the regions, whereas for magnetic and plage regions we have taken their full angular extent. Further, the excess brightness temperatures of the 3.5 and 9 mm regions is also proportional to the magnetic field strength of the plage regions; however, the fact that the mean line of Figure 3c for 3.5 mm-λ does not pass through the zero implies that a minimum magnetic field strength is required for the regions to be observable at 3.5 mm wavelength. Figures 3d and 3e show that the excess brightness temperatures at 3.5 and 9 mm are very poorly correlated with magnetic fields and areas of associated sunspots.

Only three solar maps were obtained at 1.2 mm wavelength, one on 24 September and two on 25 September, 1969. Figure 1c shows one of these maps. It is clear from this map as well as from the map of 24 September, 1969, when a 3.5 mm map was also obtained, that solar activity is much less pronounced at 1.2 mm than at longer wavelengths of 3.5 and 9 mm. Indeed the excess brightness temperatures of the regions rarely exceeds by more than 150 K the background temperature. The peaks then correspond to the stronger peaks of Ca-plage regions and the strong magnetic regions.

(2) One of the most important characteristics of most 3.5 mm and some 9 mm maps is the existence of 'temperature depressions' or 'absorption features'. These features usually correspond to dark disk filaments observed in Hα. In analogy with 'radio spots' and 'radio plages', we shall call them 'radio filaments'. As we know, the dark

filaments form in regions of zero longitudinal magnetic field; the filamentary material is supported by a magnetic field parallel to the surface of the Sun. It is relevant to note that the temperature contours between the two components of a mm-λ double source very often delineates the boundary of the neutral region of the magnetic bipolar region even when the 'radio filament' is not so obvious. Sometimes one observes radio filament without the corresponding Hα filament. This is understandable if one interprets the absorption as being caused by free-free absorption of the radio radiation by the filamentary material having high electron density and lower temperature; the optical depth is higher at radio wavelengths than in Hα, consequently one can observe radio filament even when the optical filament is absent or too old to be observable. This also explains why the absorption is found to be stronger and is observed more often at 3.5 mm than at 9 mm, since the latter radiation originates at a higher level. This interpretation leads naturally to a method of estimating the electron density in the filament from the observed amount of absorption at 3.5 mm wavelength. The mean optical depth τ is given by $\tau = Kl$, K being the absorption coefficient and l the dimension of the filamentary material through which the radio radiation passes. Since K depends upon the wavelength λ, electron density N_e and electron temperature T_e, therefore assuming an appropriate value of T_e, one can determine N_e. If one can measure the absorption at a second wavelength with comparable angular resolution, one can estimate both N_e and T_e. The measurement of absorption at a number of millimeter wavelengths should lead to a fairly good estimate of the height of the disk filaments, since at a certain wavelength the absorption will cease to be observable. Assuming $T_e = 5000$ K, $l \simeq 2000$ km (since only the linear thickness of the filamentary material is relevant for absorption of radio waves), an observed absorption of about 200 K will lead to an electron density of 5×10^{10} per cm^3. Since the 2000 km thickness of the filament may consist of a number of 'strands' of higher electron density, the mean electron density of 5×10^{10} per cm^3 estimated from absorption of millimeter waves seems quite reasonable.

(3) The properties of the slowly varying radiation at millimeter wavelengths seem to be consistent with the thermal origin of this radiation in the higher than normal density regions at chromospheric temperatures. Indeed, the spectrum of brightness temperature which decreases with decreasing wavelength is compatible with this explanation. It is quite obvious that the gyro-resonance absorption which is invoked to explain the slowly varying component at centimeter wavelengths cannot play any role at millimeter wavelengths, since the required magnetic field is at least an order of magnitude stronger than observed. This interpretation is strengthened by the fact that there is poor correlation between brightness temperature and sunspot magnetic field. The thermal radiation at millimeter wavelengths in the presence of a magnetic field should be circularly polarized; the degree of circular polarization can be used to measure the longitudinal magnetic fields in the chromosphere. Indeed for quasi-longitudinal propagation of radio waves in the magneto-ionic medium of the chromosphere, the degree of polarization is simply related to the magnetic field (see e.g. Kundu, 1965). Since the millimeter wavelength regions show one-to-one correspon-

dence with the regions of longitudinal magnetic fields on magnetograms, the assumption of quasi-longitudinal propagation seems to be justified. Thus if one can measure the degree of circular polarization at 3.5 and 9 mm-λ, one should be able to get fairly good estimates of magnetic fields at different heights in the chromosphere.

As mentioned earlier, the Sun's activity at 1.2 mm-λ is much less pronounced than at 3.5 and 9 mm-λ. This may be due to the fact that the Sun's activity at short radio wavelengths is caused by some particular magnetic field structure which is such that the main zone of activity occurs above a certain altitude, namely, above the level where the 1.2 mm-λ radiation occurs. Alternatively, one can imagine that in the region of origin of 3.5 mm wavelengths the electron temperature and density are such that the optical depth at 3.5 mm is only of the order of unity. If the T_e and N_e in the region of origin of 1.2 mm-λ do not change much, one should have lower optical depth at 1.2 mm because of shorter wavelength, and consequently the excess brightness temperature of an active region will decrease considerably. If this interpretation is correct, then at times of high activity, one might expect to see higher brightness temperatures at 1.2 mm wavelength.

Acknowledgements

I am deeply indebted to Dr. D. S. Heeschen, Director of NRAO for allowing the telescope time, and also for suggesting the use of the 1.2 mm radiometer. I express my sincere thanks to Dr. David Buhl and Mr. G. Grove for help in the preparation of the observations, and Messrs. D. Cardarella, W. Daniels and R. Hogarth for help with the observations. It is a pleasure to thank Mr. S. Y. Liu for help in the reduction of the data. This research was supported by NASA grant NGR 21-002-199.

References

Buhl, D. and Tlamicha, A.: 1970, *Astron. Astrophys.* (in press).
Kundu, M. R.: 1965, *Solar Radio Astronomy*, John Wiley – Interscience Publishers, p. 234.